Inorg. Chem. **2007**, *46*, 3810–3812

Inorganic Chemistry
Communication

Manganese(III,IV) and Manganese(III) Oxide Clusters Trapped by Copper(II) Complexes

Satoshi Yamashita,[†] Takuya Shiga,[†] Masashi Kurashina,[†] Masayuki Nihei,[†] Hiroyuki Nojiri,[‡] Hiroshi Sawa,[§] Toru Kakiuchi,[§] and Hiroki Oshio*,[†]

Graduate School of Pure and Applied Sciences, Department of Chemistry, University of Tsukuba, Tennodai 1-1-1, Tsukuba 305-8571, Japan, Institute of Material Research, Tohoku University, Katahira 2-1-1, Aoba-ku, Sendai 980-8577, Japan, and Institute of Material Research Science, High Energy Accelerator Research Organization, Oho 1-1, Tsukuba 305-0801, Japan

Received November 28, 2006

Reactions of quinquedentate Schiff base ligands with Mn and Cu ions afforded icosa- and hexadecanuclear mixed-metal clusters in which dinuclear Cu^{II} complexes trapped oxo-bridged $[Mn^{III}_8Mn^{IV}_4O_{12}]$ and $[Mn^{III}_6O_6]$ cores, respectively. Maximum entropy method analysis for synchrotron X-ray diffraction data was used to determine the oxidation states of the Mn ions.

Some solid-state oxides were endowed by nature with physical and chemical properties such as piezoelectricity, superconductivity, ferromagnetism, and catalytic activities, and these properties depend upon the crystal structures, metal ions, and tunable valency.[1] Recently, mixed-valent Mn compounds have been studied intensely because of their catalytic abilities and their solid-state properties. $LaMn^{III}O_3$, which has a Perovskite structure, is an antiferromagnetic insulator, and the material becomes a ferromagnetic conductor with sufficient hole doping.[2] On the other hand, metal oxide clusters exhibit a wealth of organic−inorganic hybrid materials such as photosystem II[3] and quantum-spin systems.[4] Oxo-bridged Mn dimers and tetramers have been shown to mimic water oxidation in biological systems,[5] and a dodecanuclear Mn−O cluster is the first single-domain magnet called a single-molecule magnet.[4] Manganese oxide clusters have been prepared by using ambient and solvothermal synthetic techniques, in which manganese acetate has been the most frequently used starting materials.[6] Some new synthetic routes, such as the reduction of MnO_4^-, have been reported.[7] However, the number of rational routes for preparing manganese oxide clusters is still limited. It is noted that structures and properties can be dramatically influenced and tunable by synthetic conditions and that mixed-valent metal ions play important roles in their properties. Oxidation states of metal ions can be assigned by using charge considerations, coordination bond lengths, and bond-valence-sum (BVS) calculations.[8] However, determination of the oxidation states of metal ions, which have nonlocalized valence electrons, is rather difficult. We report here a new synthetic route to manganese oxide clusters and determination of the oxidation states of Mn ions by using the maximum entropy method (MEM) for X-ray diffraction data.

The reaction of a quadridentate Schiff base (H_3bemp = 2,6-bis[*N*-(2-hydroxyethyl)iminomethyl]-4-methylphenol)[9] with $Mn(NO_3)_2{\cdot}6H_2O$ and $Cu(OAc)_2{\cdot}H_2O$ in a 1:2:$^2/_3$ ratio afforded the heterometal cluster of $[Mn^{III}_8Mn^{IV}_4Cu^{II}_8O_{16}(OMe)_4(OAc)_4(NO_3)_2(bemp)_4(H_2O)_{10}](NO_3)_2{\cdot}8H_2O$ (**1**), while the reaction with a 1:2:2 ratio yielded the different cluster $[Mn^{III}_6Cu^{II}_{10}O_8(OH)_2(OAc)_8(bemp)_2(Hbemp)_2](NO_3)_2{\cdot}14H_2O$ (**2**).[10] A dark-brown crystal of **1** crystallizes in the tetragonal space group $I4_1/amd$.[11] A complex cation of **1** has S_4 symmetry and contains four dinuclear Cu units ($[Cu^{II}_2$-

---

* To whom correspondence should be addressed. E-mail: oshio@chem.tsukuba.ac.jp.

[†] University of Tsukuba.

[‡] Tohoku University.

[§] High Energy Accelerator Research Organization.

(1) Hagrman, P. J.; Hagrman, D.; Zubieta, J. *Angew. Chem., Int. Ed.* **1999**, *38*, 2638.

(2) (a) Bednorz, J. G.; Müller, K. A. *Z. Phys. B* **1986**, *64*, 189. (b) Tokura, Y.; Nagaosa, N. *Science* **2000**, *288*, 462. (c) Millis, A. J. *Nature* **1998**, *392*, 147.

(3) (a) Christou, G. *Acc. Chem. Res.* **1989**, *22*, 328. (b) Wieghardt, K. *Angew. Chem., Int. Ed. Engl.* **1994**, *33*, 725. (c) Debus, R. J. *Biochem. Biophys. Acta* **1992**, *1102*, 269. (d) Brudvig, G. W.; Thorp, H. H.; Crabtree, R. H. *Acc. Chem. Res.* **1991**, *24*, 311.

(4) Christou, G.; Gatteschi, D.; Hendrickson, D. N.; Sessoli, R. *MRS Bull.* **2000**, *25* (11), 66.

(5) (a) Bossek, U.; Weyhermüller, T.; Wieghardt, K.; Nuber, N.; Weiss, J. *J. Am. Chem. Soc.* **1990**, *112*, 6387. (b) Yocum, C. F.; Pecoraro, V. L. *Curr. Opin. Chem. Biol.* **1999**, *3*, 182. (c) Ruettinger, W.; Yagi, M.; Wolf, K.; Bernasek, S.; Dismukes, G. C. *J. Am. Chem. Soc.* **2000**, *122*, 10353. (d) Mukhopadhyay, S.; Staples, R. J.; Armstrong, W. H. *Chem. Commun.* **2002**, 864. (e) Bhaduri, S.; Pink, M.; Christou, G. *Chem. Commun.* **2002**, 2352.

(6) (a) Sun, Z.; Gantzel, P. K.; Hendrickson, D. N. *Inorg. Chem.* **1996**, *35*, 6640. (b) King, P.; Wernsdorfer, W.; Abboud, K. A.; Christou, G. *Inorg. Chem.* **2004**, *43*, 7315.

(7) (a) Parsons, S.; Smith, A. A.; Winpenny, R. E. P. *Chem. Commun.* **2000**, 579. (b) Eshel, M.; Bino A. *Inorg. Chim. Acta* **2002**, *329*, 45. (c) Beattie, J. K.; Hambley, T. W.; Klepetko, J. A.; Masters, A. F.; Turner, P. *Polyhedron* **1997**, *16*, 2109.

(8) Thorp, H. H. *Inorg. Chem.* **1992**, *31*, 1585.

(9) Zhang, W. X.; Ma, C. Q.; Wang, X. N.; Yu, Z. G.; Lin, Q. J.; Jiang, D. H. *Chin. J. Chem.* **1995**, *13*, 497.

10.1021/ic062258h CCC: $37.00

© 2007 American Chemical Society
Published on Web 04/14/2007

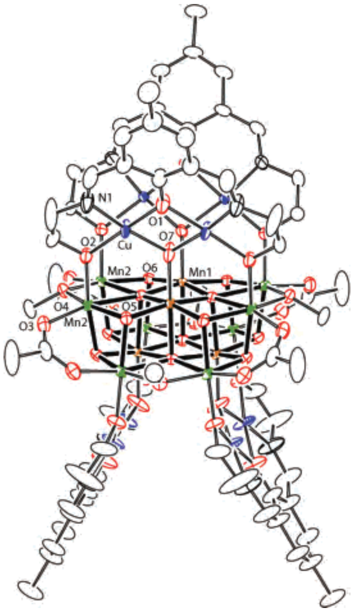

Figure 1. ORTEP diagram of cation **1**. Green, brown, and blue ellipsoids correspond to Mn^{III}, Mn^{IV}, and Cu^{II} ions, respectively. Coordinating water molecules and nitrate ions are omitted for clarity.

(bemp)]) capping a pentacubic core of manganese oxide, $[Mn^{III}_8Mn^{IV}_4(\mu_3\text{-}O)_8(\mu_5\text{-}O)_4]$ (Figure 1). The manganese oxide core, which is composed of 12 Mn ions bridged by 4 μ_5-O^{2-} (O5) and 8 μ_3-O^{2-} (O6) ions, has five face-shared cubes arranged in a cross shape. Four $[Cu^{II}_2(\text{bemp})]$ units cap the oxide core on its top and bottom faces via μ_3-O^{2-} (O7) and μ_2-alkoxo (O2) bridges, and four acetate ions and four methoxide ions surround the core. Cu^{II} ions in the $[Cu^{II}_2(\text{bemp})]$ unit are doubly bridged by μ_2-phenoxo (O1) and μ_3-O^{2-} (O7) bridges, and each Cu^{II} ion has elongated octahedral coordination geometry. The equatorial sites of the Cu^{II} ions were coordinated by N_1O_3 atoms from bemp^{3-} and μ_3-O^{2-} (O7) ions, and the axial sites were occupied either by two water molecules or by one water molecule and a NO_3^- ion. The NO_3^- ions were positionally disordered with 50% probability and completed the sixth coordination site on one of the two Cu^{II} ions. Bond lengths about Cu^{II} ions are in the range of 1.912(5)−1.947(3) and 2.493(6)−2.736(6) Å for equatorially and axially coordinating atoms, respectively. The six coordination sites of the Mn1 ion are occupied by oxide ions, while each Mn2 ion has six coordinating O atoms from three oxide, methoxide, alkoxide, and acetate ions. Coordination bond lengths about Mn1 and Mn2 are in the range of 1.919(6)−2.120(4) and 1.912(3)−2.326(3) Å, respectively, and the average coordination bond length ($d_{av} = 1.968$ Å) of the Mn1 ion is shorter than that ($d_{av} = 2.033$ Å) of the Mn2 ion. BVS calculations yielded values of 3.42 and 3.07 for Mn1 and Mn2, assuming Mn^{IV} and Mn^{III}, respectively. The structural data suggest that the Mn1 ions have higher oxidation states than the Mn2 ions. It is noted that the X-ray absorption near-edge structure (XANES) spectrum for **1** consists of the superimposed spectra characteristic of Mn^{III} and Mn^{IV} ions (Figure 1S in the Supporting Information). We applied the MEM analysis for the synchrotron X-ray diffraction data[11] to obtain further information about the oxidation states of Mn ions.[12] Contour maps of the electron density reproduced from the MEM are depicted in Figure 2. The number of electrons on the Mn1 and Mn2 ions were computed to be 19.9 and 20.3, respectively, by using the Voronoi deformation density method,[13] suggesting that Mn1 has a higher oxidation number than Mn2. It is noted that electron-counting analyses are affected by the diffuseness of the outer shells, and the obtained values are sometimes less than the ones predicted by the formal oxidation state. [14] We tentatively assigned the oxidation states

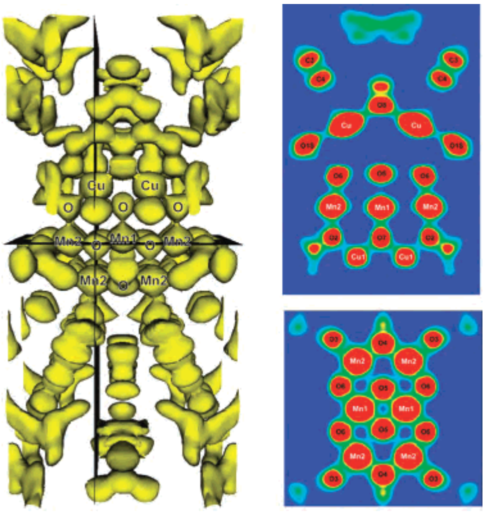

Figure 2. MEM electron-density distribution in the oxide core of **1**: horizontal (right bottom) and vertical (right up) divisions were taken from planes of the whole molecule (left). The contour maps are drawn from 0.001 to 2.0 e $Å^{-3}$, and high electron density is colored in red.

---

(10) A mixture of $Mn(NO_3)_2\cdot 6H_2O$ (287 mg, 1.0 mmol) and $H_3\text{bemp}$[9] (125 mg, 0.5 mmol) in methanol (10 mL) was stirred at 60 °C for 20 min, and the solution turned reddish brown. To the resulting solution were added triethylamine (152 mg, 1.5 mmol) and $Cu(OAc)_2\cdot H_2O$ (67 mg, 0.3 mmol), and the resulting solution was heated at 60 °C for 20 min. The solution was allowed to stand for several days, and dark-brown columnar crystals of **1** were obtained (yield: 23%). Anal. Calcd for the dried sample, $C_{64}H_{104}Cu_8Mn_{12}N_{12}O_{62}$: C, 24.01; H, 3.27; N, 5.25. Found: C, 24.02; H, 2.99; N, 5.24. Complex **2** was synthesized similarly to **1** except for the amount of $Cu(OAc)_2\cdot H_2O$ (200 mg, 1.0 mmol) that was used. Dark-brown lozenge crystals were obtained from the reaction mixture (yield: 21 %). Anal. Calcd for the dried sample, $C_{68}H_{104}Cu_{10}Mn_6N_{10}O_{52}$: C, 28.60; H, 3.67; N, 4.90. Found: C, 28.40; H, 3.38; N, 5.15.

(11) Crystal data for **1**: $C_{64}H_{84}N_{12}Cu_8Mn_{12}O_{70}$, tetragonal $I4_1/amd$, $a = 24.702(2)$ Å, $c = 20.365(3)$ Å, $V = 12427(2)$ $Å^3$, $Z = 4$, $d_{calcd} = 1.769$ Mg m^{-3}, $T = 100$ K, λ(synchrotron) = 1.000 00 Å, 18 848 reflections measured, 3979 unique reflections ($R_{int} = 0.0310$). Final R1 = 0.0690 and wR2 = 0.2169 [$I > 2\sigma(I)$]. X-ray diffraction data were obtained with a Weissenberg-type imaging plate detector. Crystal data for **2**: $C_{68}H_{88}Cu_{10}Mn_6N_{10}O_{58}$, dark-brown lozenge (0.4 × 0.15 × 0.1 mm^3), $M = 2938.55$, triclinic $P\bar{1}$, $a = 14.208(3)$ Å, $b = 14.344(3)$ Å, $c = 15.912(3)$ Å, $\alpha = 77.549(3)°$, $\beta = 64.388(3)°$, $\gamma = 75.093(4)°$, $V = 2805.5(9)$ $Å^3$, $Z = 1$, $d_{calcd} = 1.739$ Mg m^{-3}, $T = 200$ K, λ(Mo Ka) = 0.710 73 Å, 12 885 reflections measured, 7993 unique reflections ($R_{int} = 0.0226$). Final R1 = 0.0570 and wR2 = 0.1697 using reflections with $I > 2\sigma(I)$.

(12) MEM analysis was performed with the Enigma program (Tanaka, H.; Tanaka, M.; Nishibori, E.; Kato, K.; Iishi, T.; Sakata, M. *J. Appl. Crystallogr.* **2002**, *35*, 282) at a resolution of 128 × 128 × 128 pixels, and the *R* factor of the final MEM charge density was 0.046.

(13) Electron counting on each Mn ion was performed within the particular compartment of the space (Voronoi cell), which was defined as a region surrounded by perpendicular bisecting planes of bonds between Mn and neighboring O nuclei. Guerra, C. F.; Handgraaf, J.-W.; Baerends, E. J.; Bicelhaupt, F. M. *J. Comput. Chem.* **2004**, *25*, 189.

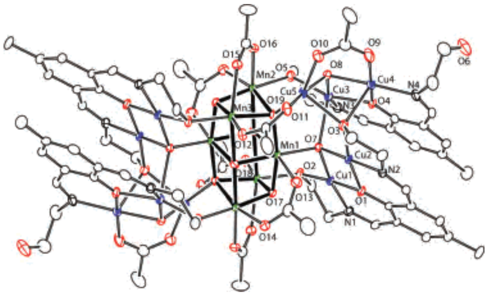

Figure 3. ORTEP diagram of cation **2**. Green and blue ellipsoids correspond to Mn^{III} and Cu^{II} ions, respectively.

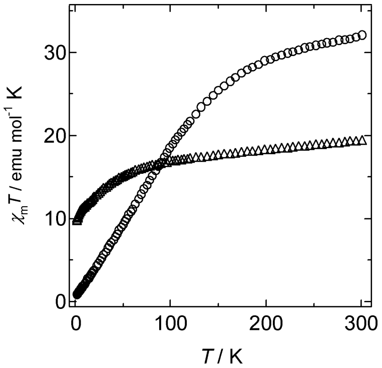

Figure 4. $\chi_m T$ vs T plots of (○) **1** and (△) **2**.

of Mn1 and Mn2 to Mn^{IV} and Mn^{III} ions, respectively. The exact number of electrons on Mn atoms cannot be determined from the present MEM analysis; hence, the localization or delocalization of the valence electrons is not clear.

Complex **2** crystallized in triclinic space group $P\bar{1}$. The complex cation of **2** is located on a crystallographic inversion center and has a face-sharing double cube ($[Mn^{III}_6(\mu_3\text{-}O)_4(\mu_4\text{-}O)_2]$), four dinuclear units ($[Cu^{II}_2(\text{bemp})]$), and two additional mononuclear Cu^{II} units linking the former two units (Figure 3). Charge consideration and coordination bond lengths suggested that Mn1−Mn3 are Mn^{III} ions. The double cube was comprised of six Mn^{III} ions with two $\mu_4\text{-}O^{2-}$ (O18) and four $\mu_3\text{-}O^{2-}$ (O17) ions. Coordination bond lengths about Mn1, Mn2, and Mn3 ions are 1.878(5)−2.179(6), 1.892(5)−2.392(6), and 1.896(5)−2.258(5) Å, respectively, and apparent Jahn−Teller elongations were observed along with O13−Mn1−O18, O14−Mn2−O19*, and O15−Mn3−O18* vectors. Two acetate ions and $[Cu^{II}_2(\text{bemp})]$ units cap the double cube via $\mu_4\text{-}O^{2-}$ (O7) and $\mu_2\text{-}O^{-}$ (O5 or O2) bridges, and an additional mononuclear Cu^{II} unit bridges the double-cube and $[Cu^{II}_2(\text{bemp})]$ units. In the $[Cu^{II}_2(\text{bemp})]$ units, Cu1 and Cu2 ions have square-planar geometry, with each having N_1O_3 chromophores, and they are doubly bridged by $\mu_4\text{-}O^{2-}$ (O7) and μ_2-phenoxo (O1 from bemp^{3-}) ions. Cu3 and Cu4 ions, on the other hand, have square-pyramidal coordination geometry with N_1O_4 chromophores, of which the equatorial sites are occupied by one N atom and three O atoms from bemp^{3-}. The apical positions are occupied by μ_3-alkoxo (O3) and $\mu_4\text{-}O^{2-}$ (O7) groups, bridging to the neighboring dinuclear units. Cu5 in the mononuclear unit has a square-pyramidal coordination geometry with five O atoms and is bridged with Cu3 and Cu4 by $\mu_3\text{-}OH^{-}$ (O8) groups. The monocopper unit links the double-cube and $[Cu^{II}_2(\text{bemp})]$ units via two $\mu_2\text{-}AcO^{-}$, $\mu_3\text{-}OH^{-}$ (O8), and $\mu_3\text{-}O^{-}$ (O3 from bemp^{3-}) groups.

Magnetic susceptibility measurements for **1** and **2** were carried out in the temperature range of 1.8−300 K (Figure 4). The $\chi_m T$ values at 300 K for **1** and **2** were 32.1 emu mol^{-1} K and 19.4 emu mol^{-1} K, which were smaller than the values expected for the magnetically uncorrelated components of $Mn^{IV}_4Mn^{III}_8Cu^{II}_8$ (34.5 emu mol^{-1} K for $g = 2.0$) and $Mn^{III}_6Cu^{II}_{10}$ (21.7 emu mol^{-1} K for $g = 2.0$), respectively. The Cu^{II} ions in $[Cu^{II}_2(\text{bemp})]$ units are antiferromagnetically coupled through phenoxo, oxo, and hydroxo bridges, and their coupling constants sometimes exceeded $J = -100$ cm^{-1}.[15] The contribution of the Cu^{II} ions to the $\chi_m T$ values is, therefore, negligibly small in the low-temperature region. The Weiss (Curie) constants obtained by using the data above 200 K were −72.6 K (39.8 emu mol^{-1} K) and −44.6 K (22.0 emu mol^{-1} K) for **1** and **2**, respectively. A gradual decrease of the $\chi_m T$ values as the temperature was lowered suggests that antiferromagnetic interactions are operated also among the Mn centers via oxide bridges.

The MEM analysis for the synchrotron X-ray diffraction data has been applied to determine small guest−gas molecules trapped in cage fullerene and porous coordination polymers.[16] The MEM analysis is also useful tool to evaluate the electron density of mixed-valent $Mn^{III,IV}$ systems. In summary, combinations of Mn and Cu ions with quinquedentate Schiff base ligands give a new synthetic route to prepare large Mn−O clusters. Ligand modifications, subtle changes in the reaction conditions, and different combinations of metal ions may provide opportunities to prepare larger molecules with different core structures.

Acknowledgment. This work was supported by a Grant-in-Aid for Scientific Research from the Ministry of Education, Science, Sports and Culture, Japan, and by the COE and TARA projects at University of Tsukuba.

Supporting Information Available: Crystallographic details in CIF format and XANES spectra (Figure 1S). This material is available free of charge via the Internet at http://pub.acs.org.

IC062258H

---

(14) Koritsanszky, T. S.; Coppens, P. *Chem. Rev.* **2001**, *101*, 1583.

(15) Mukherjee, S.; Weyhermüller, T.; Bothe, E.; Wieghardt, K.; Chaudhuri, P. *Eur. J. Inorg. Chem.* **2003**, 863.

(16) (a) Sawa, H.; Wakabayashi, Y.; Murata, Y.; Murata, M.; Komatsu, K. *Angew. Chem., Int. Ed.* **2005**, *45*, 1981. (b) Kitaura, R.; Kitagawa, S.; Kubota, Y.; Kobayashi, T.; Kindo, K.; Mita, Y.; Matsuo, A.; Kobayash, M.; Chang, H.-C.; Ozawa, T.; Suzuki, M.; Sakata, M.; Takata, M. *Science* **2002**, *298*, 2385.